Dynamics of sandwich curved beams with viscoelastic core described by fractional derivative operators

Marcelo T. Piovan, Rubens Sampaio, Jean-François Deü

DYNAMICS OF SANDWICH CURVED BEAMS WITH VISCOELASTIC CORE DESCRIBED BY FRACTIONAL DERIVATIVE OPERATORS

Marcelo T. Piovan[a], **Rubens Sampaio**[b] **and Jean-François Deü**[c]

[a]*Research Center for Theoretical and Applied Mechanics, Universidad Tecnológica Nacional FRBB. 11 de Abril 461, B8000LMI, Bahía Blanca. Argentina, mpiovan@frbb.utn.edu.ar,*
http://www.frbb.utn.edu.ar

[b]*Departament of Mechanical Engineering. Pontifícia Universidade Católica do Rio de Janeiro. Rua Marquês de São Vicente 225, Rio de Janeiro RJ-22453-90, Brazil, rsampaio@puc-rio.br,*
http://www.mec.puc-rio.br

[c]*Structural Mechanics and Coupled Systems Laboratory , Conservatoire Nationale des Arts et Métiers (CNAM), 2 rue Conté, 75003 Paris. France, jean-francois.deu@cnam.fr, http://www.cnam.fr/lmssc*

Keywords: Sandwich curved beams, viscoelastic damping, fractional derivatives, dynamic analysis.

Abstract. This paper presents a finite element formulation for transient dynamic analysis of sandwich curved beams with embedded viscoelastic material whose constitutive behavior is modeled by means of fractional derivative operators. The sandwich configuration is composed of a band as a viscoelastic core bonded to elastic metallic strips. The viscoelastic model used to describe the behavior of the core is a four-parameter fractional derivative model. The Grünwald definition of the fractional operator is used to implement the viscoelastic model into a finite element formulation. Then, discretized motion equations are solved with a direct time integration scheme based on the Newmark method. A useful aspect of the procedure is that only the anelastic displacements history is kept. This allows an important save of computational resources associated with the non-locality of the operators for fractional derivatives. Numerical studies are presented in order to validate the curved beam model with other approaches (frames of straight beams) as well as to analyze the influence of different parameters in the transient dynamics of naturally curved sandwich beams.

1 INTRODUCTION

In recent years the research community has manifested a sound interest in the investigation of dynamic behavior of slightly damped structures. Many researchers have shown that the employment of viscoelastic materials can improve the dynamics of such structures. These materials can be incorporated into different types of structures by means of a number of methods and techniques. For example, a common and well known treatment to reduce structural vibrations is the constrained layer passive damping technique that is usually employed together with schemes of active control (Baz, 1997; Trindade et al., 2001).

The viscoelastic solids are known to manifest a certain dependence of their dynamic properties with respect to the vibration frequency in a broad frequency range (Coronado et al., 2002). This feature leads to the problem of the proper characterization of the damping properties of such material. The classical models for linear viscoelastic solids, based on integer derivative operators or convolution integrals or internal variables, have a complicated application due to the important amount of parameters to characterize the material behavior. Under this circumstances the employment of viscoelastic models based on fractional derivatives applied to both strains and stresses offer interesting simplification alternatives.

The use of the fractional derivative concept, in the context of viscoelasticity, was commonly applied as an effective technique for curve-fitting of experimental data. Bagley and Torvik (1983) developed a one-dimensional model for a viscoelastic material using fractional derivative operators. Since then, this model for viscoelastic solids was incorporated in many structural applications (Galucio et al., 2004) as well as specific implementation of fractional constitutive models into computational procedures such finite elements. In this context, the numerical methods in the time domain are generally associated with the Grünwald definition for the fractional order derivative of the stress-strain relation in conjunction with a time discretization scheme (see e.g. Padovan (1987)). The finite element formulation proposed by Enelund and Jossefson (1997) employs the fractional calculus involving convolution integral description with a singular kernel function of Mittag-Leffler type. Galucio et al. (2004) developed a finite element formulation to analyze the transient dynamics of a sandwich beam with viscoelastic embedded layer whose material behavior was modeled with fractional derivative operators. They used the four-parameters model of Bagley and Torvik (1983) to characterize the frequency-dependence of the viscoelastic layer. Most of the aforementioned works are restricted to bar models or straight beam models as well as one degree of freedom models, but none of them is dedicated to analyze the transient dynamics of common but more complex structures such as curved beams.

Studies on the dynamics of naturally curved beams deserved the attention of no few researchers in the very recent years, specially in layered configurations. Baba and Thoppul (2009), among others, carried out experimental studies on the dynamics of sandwich composite curved beams with cracks and debonded interfaces. Sunsanto (2009) analyzed the dynamics of layered curved beams with piezoelectric skins by means of the Rayleigh-Ritz method. To the authors' knowledge there are no reports concerning the dynamic of sandwich curved beams with embedded viscoelastic materials whose frequency-dependence behavior is modeled with fractional derivative operators. Thus, in the present work a new model introduced and a numerical formulation based in the method of finite elements is developed in order to study the transient dynamics of sandwiched viscoelastic curved beams. The curved structure is composed by two elastic layers covering a viscoelastic core, which is modeled with the formalism of Bagley and Torvik (1983). The viscoelastic core is assumed to be shear deformable for flexure whereas the outer layers keep the conventional assumptions of Bernoulli-Euler modeling but applied to a

beam with curved axis. Higher order curvature effects are disregarded assuming the structure as a slim and shallow curved beam.

Numerical studies are carried out in order to analyze modeling features such as the effects of truncation, solution convergence aspects, and validation and comparison with other approaches in the literature as well. Other set of studies are devoted to analyze the influence of different geometric and material parameters in the transient dynamics of viscoelastic sandwich curved beams.

2 STRUCTURAL MODEL DEVELOPMENT

2.1 Model assumptions

In Figure 1 one can see a sketch of curved structural member. The beam is made of two elastic layers (numbered as 1 and 2) that cover a viscoelastic core (identified with number 3). A global circumferential reference system located at point O is employed. The beam is constrained to move only in the plane XY, consequently no out-of-plane motions are involved. In order to construct the dynamic model of a sandwich curved beam, the following assumptions are considered:

(1) The elastic layers are perfectly bonded to the viscoelastic one.

(2) The bending shear deformability is considered only in the viscoelastic layer but neglected in the elastic ones.

(3) A plane stress state is assumed for all layers.

(4) The longitudinal elastic modulus and the shear elastic modulus of the viscoelastic core are proportional (this implies that Poisson coefficient is frequency-independent).

(5) The structure is featured as a shallow circular curved beam.

(6) The ratio of the thickness to the curvature radius is small, consequently no higher order effects due to curvature are considered.

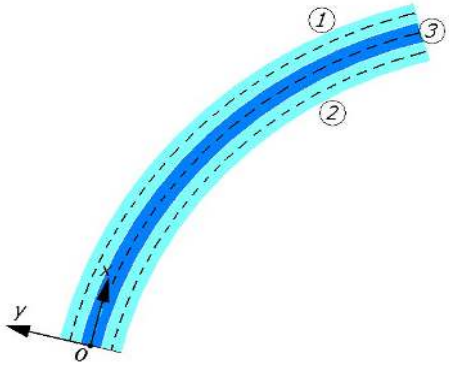

Figure 1: Beam configuration.

2.2 Kinematic description

Taking into account the aforementioned assumptions the displacement field for a sandwich curved beam can be written in the following form (Piovan and Cortínez, 2007):

$$\begin{aligned} u_{xi}(x,y,t) = &\quad u_i(x,t) - (y-y_i)(\theta_i(x,t) - u_i(x,t)/R_i) \\ u_{yi}(x,y,t) = &\quad v(x,t) \end{aligned} \tag{1}$$

where the subscript $i = 1, 2, 3$ stands for upper, lower and inner layer, respectively. u_{xi} and u_{yi} are the axial and transverse displacements of each layer, u_i are the axial (or circumferential) displacement of the center line of each layer (these entities can be understood more clearly by observing Figure 2). θ_i are the bending rotation of each layer measured from the corresponding centerlines of each layer. v is the transverse (or radial) displacement that is common for all the layers. y_i are the distance between middle lines of adjacent layers, whereas R_i are the curvature radius at the center line of each layer.

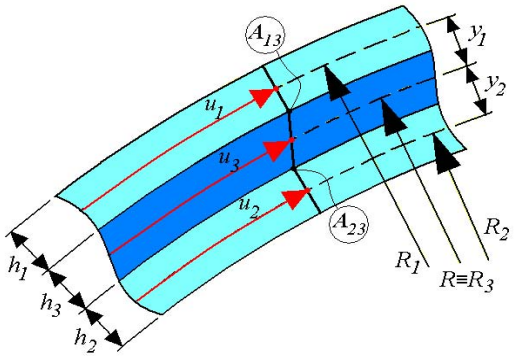

Figure 2: Detail of the curved beam showing the main displacements.

According to the assumptions (2) to (5) and taking into account the condition of continuity of the displacement field in the interfaces A_{13} and A_{23} as shown in Figure 2, one can obtain the displacements of the viscoelastic core in terms of the displacements of the elastic outer layers. The bending rotation of the outer layers is assumed to be the same for both layers. The axial displacement and the rotation in the centerline of the viscoelastic core can be written in the following form:

$$\begin{aligned} u_3 = &\quad \frac{u_1+u_2}{2} + v'\frac{h_1-h_2}{4} - \frac{h_1u_1}{4R_1} + \frac{h_2u_2}{4R_2}, \\ \theta_3 = &\quad \frac{u_2-u_1}{h_3} - \frac{h_1+h_2}{2h_3} + \frac{h_2u_2}{2h_3R_2} + \frac{h_1u_1}{2h_3R_1} + \\ &\quad \frac{u_1+u_2}{2R_3} + v'\frac{h_1-h_2}{4R_3} - \frac{h_1u_1}{4R_3R_1} + \frac{h_2u_2}{4R_3R_2}, \end{aligned} \tag{2}$$

where h_i are the thicknesses of the corresponding layers. The curvature radius R_i are:

$$\begin{aligned} R_1 = R + y_1 = R + (h_3+h_1)/2, \\ R_2 = R - y_2 = R - (h_3+h_2)/2, \\ R_3 = R. \end{aligned} \tag{3}$$

Now introducing the mean and relative axial (or circumferential) displacements defined in Eq. (4), one can redefine all displacement as in Eq. (5).

$$\bar{u} = \frac{u_1 + u_2}{2}, \qquad \tilde{u} = u_1 - u_2, \tag{4}$$

$$\begin{aligned} u_1 &= \bar{u} + \frac{\tilde{u}}{2}, \qquad u_2 = \bar{u} - \frac{\tilde{u}}{2} \\ \theta_1 &= v', \qquad \theta_2 = v', \\ u_3 &= \bar{u} + v'\frac{\tilde{h}}{4} - \frac{h_1}{4R_1}\left(\bar{u} + \frac{\tilde{u}}{2}\right) + \frac{h_2}{4R_2}\left(\bar{u} - \frac{\tilde{u}}{2}\right), \\ \theta_3 &= -\frac{\tilde{u}}{h_3} - \frac{v'\bar{h}}{h_3} + \frac{v'\tilde{h}}{4R} + \frac{\bar{u}}{R} + \frac{h_1}{2h_3R_1}\left(\bar{u} + \frac{\tilde{u}}{2}\right) + \frac{h_2}{2h_3R_2}\left(\bar{u} - \frac{\tilde{u}}{2}\right), \end{aligned} \tag{5}$$

where for the sake of notation simplicity apostrophes mean derivation with respect to the variable x. $\bar{h}$ and $\tilde{h}$ are defined by:

$$\bar{h} = \frac{h_1 + h_2}{2}, \qquad \tilde{h} = h_1 - h_2. \tag{6}$$

Notice that when the condition $R \to \infty$ the displacement field given in Eq. (5) reduces to the case of a straight beam developed by Galucio et al. (2004) and Trindade et al. (2001).

2.3 Strain-displacement relations

The strain-displacement relationship defined according to the circumferential reference system adopted for the curved beam can be written as:

$$\begin{aligned} \varepsilon_{xxi} &= \left(\frac{\partial u_{xi}}{\partial x} + \frac{u_{yi}}{R}\right)\mathcal{F}, \\ \gamma_{xyi} &= \left(\frac{\partial u_{yi}}{\partial x} - \frac{u_{xi}}{R}\right)\mathcal{F} + \frac{\partial u_{xi}}{\partial y}, \end{aligned} \tag{7}$$

where $\mathcal{F} = R/(R+y)$. However taking into account the assumptions (5) and (6), one gets $\mathcal{F} \approx 1$. It should be remembered that due to assumption (2), $\gamma_{xy1} = \gamma_{xy2} = 0$, and γ_{xy3} is the only relevant component of the shear strain of the beam.

Now, substituting Eq. (1) into Eq. (7) the following expressions are reached:

$$\begin{aligned} \varepsilon_{xxi} &= \varepsilon_{D1i} - (y - y_i)\varepsilon_{D2i}, \\ \gamma_{xy3} &= \varepsilon_{D33}, \end{aligned} \tag{8}$$

where, ε_{D1i} and ε_{D2i} are the membrane strains and bending curvatures of each layer, respectively; whereas ε_{D33} is the shear deformation of the viscoelastic core. Taking into account the definitions of Eq. (4) and Eq. (6), ε_{D1i}, ε_{D2i} and ε_{D33} can be written in the following form:

$$\varepsilon_{D11} = \left(\bar{u}' + \frac{\tilde{u}'}{2}\right) + \frac{v}{R_1}, \qquad \varepsilon_{D21} = -v'' + \frac{1}{R_1}\left(\bar{u}' + \frac{\tilde{u}'}{2}\right), \tag{9}$$

$$\varepsilon_{D12} = \left(\bar{u}' - \frac{\tilde{u}'}{2}\right) + \frac{v}{R_2}, \qquad \varepsilon_{D22} = -v'' + \frac{1}{R_2}\left(\bar{u}' - \frac{\tilde{u}'}{2}\right), \tag{10}$$

$$
\begin{aligned}
\varepsilon_{D13} = &\ \bar{u}'\left(1-\frac{h_1}{4R_1}+\frac{h_2}{4R_2}\right)-\frac{\tilde{u}'}{2}\left(\frac{h_1}{4R_1}+\frac{h_2}{4R_2}\right)+\frac{v''\tilde{h}}{4}+\frac{v}{R_3},\\
\varepsilon_{D23} = &\ \frac{\tilde{u}'}{h_3}\left(1-\frac{h_1}{4R_1}+\frac{h_2}{4R_2}\right)+\frac{\bar{h}}{h_3}v''-\frac{\bar{u}'}{2h_3}\left(\frac{h_1}{R_1}+\frac{h_2}{R_2}\right),\\
\varepsilon_{D33} = &\ \frac{\tilde{u}}{h_3}\left(1+\frac{h_1}{4R_1}-\frac{h_2}{4R_2}\right)+v'\left(1+\frac{\bar{h}}{h_3}+\frac{\tilde{h}}{R_3}\right)+\frac{\bar{u}}{R_3}+\frac{\bar{u}}{2h_3}\left(\frac{h_1}{R_1}+\frac{h_2}{R_2}\right).
\end{aligned}
\tag{11}
$$

If $h_1 = h_2 = 0$ and $R \to \infty$ the previous Eq. (11) corresponds to a simple straight shear deformable (or Timoshenko) beam.

2.4 Constitutive description of a viscoelastic layer

The viscoelastic behavior of the core can be described by the one-dimensional constitutive model of Bagley and Torvik (1983):

$$
\sigma(t)+\tau^{\alpha}\frac{d^{\alpha}\sigma(t)}{dt^{\alpha}} = E_o\varepsilon(t)+\tau^{\alpha}E_{\infty}\frac{d^{\alpha}\varepsilon(t)}{dt^{\alpha}},
\tag{12}
$$

where σ and ε are the stress and the strain, respectively. The following four parameters E_o, E_∞, τ and α are the relaxed elastic modulus, the non-relaxed elastic modulus, the relaxation time and the fractional derivation order, respectively.

The definition of the fractional derivative of a certain function $f(t)$ is given by the following expression introduced by Riemman-Liouville:

$$
\frac{d^{\alpha}f(t)}{dt^{\alpha}} = \frac{1}{\Gamma(1-\alpha)}\frac{d}{dt}\int_0^t \frac{f(s)}{(t-s)^{\alpha}}ds,
\tag{13}
$$

where Γ is the gamma function. The fractional order α is such that $0 < \alpha < 1$.

This four-parameter constitutive model has been shown to be an efficient tool to represent the frequency dependence of many viscoelastic materials as one can see in the works of Bagley and Torvik (1983) and Pritz (1996).

A given viscoelastic material can effectively characterized if the four parameters E_o, E_∞, τ and α are identified. There are several experimental ways to identify these parameters, for example by means of transient or harmonic dynamic tests one can obtain the longitudinal elastic modulus (by traction and/or compression), on the other hand the shear elastic modulus can be obtained by means of torsional tests.

The characterization of material parameters of the viscoelastic model can be performed by applying the Fourier Transform to the Eq. (12), obtaining the following elastic complex modulus:

$$
\hat{E}(\omega) = \frac{\hat{\sigma}(\omega)}{\hat{\varepsilon}(\omega)} = \frac{E_o+E_{\infty}(i\omega\tau)^{\alpha}}{1+(i\omega\tau)^{\alpha}}
\tag{14}
$$

where $\hat{\sigma}$ and $\hat{\varepsilon}$ are the Fourier transforms of $\sigma(t)$ and $\varepsilon(t)$, respectively. The variation of $\hat{E}(\omega)$ is bounded by two values (see Figure 3), i.e. the static modulus of elasticity, E_o (with $\omega \to 0$) and the high frequency elastic modulus, E_∞ (with $\omega \to \infty$). These parameters are such that $E_o < E_\infty$, for $\tau > 0$ and $0 < \alpha < 1$. From the real and imaginary parts of Eq. (14) it is possible to obtain the expression for the storage modulus $E_1(\omega)$ and loss modulus $E_2(\omega)$, which are

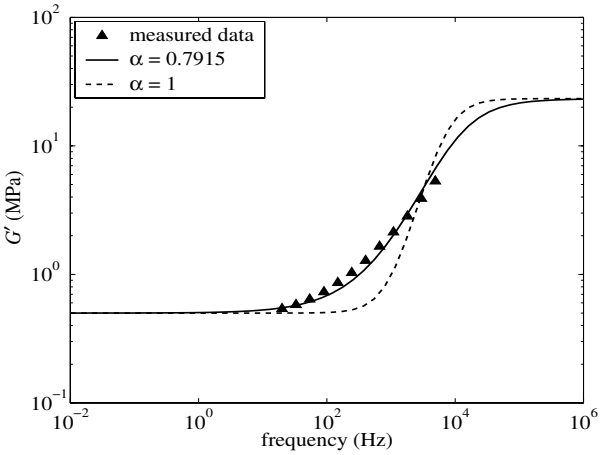

Figure 3: Beam configuration.

employed to calculate the mechanical loss factor $\eta(\omega) = E_2(\omega)/E_1(\omega)$ that fits experimental results.

The order of the fractional derivative can be obtained by assuming the values of storage modulus $E_1(\omega)$, i.e. E_o and E_∞ and the maximum mechanical loss factor (obtained from experiments). Finally the relaxation time τ can be estimated by minimization of difference between theoretical and experimental data of the complex modulus $\hat{E}(\omega)$. A more detailed explanation of this identification procedure can be followed in the work of Galucio et al. (2004). Notice that in Figure 3 the classical Zenner model (i.e. with $\alpha = 1$)) is included for comparison purposes. This makes evident how effective is the fractional derivative approach to correlate the frequency dependence of the storage modulus.

3 VARIATIONAL FORMULATION

The dynamic equations of the curved sandwich beam are derived from the Hamilton's principle:

$$\int_{t_1}^{t_2} (\delta T - \delta U + \delta W)\, dt = 0 \tag{15}$$

where δW is the variation of the work done by external forces acting on the beam. δT is the variation of the kinetic energy and δU is the variation of the strain energy. The variation of strain and kinetic energies can be written as:

$$\delta U = \sum_{i=1}^{3} \delta U_i, \qquad \delta T = \sum_{i=1}^{3} \delta T_i \tag{16}$$

where according to the assumptions:

$$\begin{aligned}
\delta T_i = & -\int_V \rho_i \left(\ddot{u}_{xi}\delta u_{xi} + \ddot{u}_{yi}\delta u_{yi}\right) dV \quad \forall i = 1,2,3, \\
\delta U_i = & \int_V \sigma_{xi}\delta\varepsilon_{xxi} dV \quad \forall i = 1,2, \\
\delta U_3 = & \int_V \left(\sigma_{x3}\delta\varepsilon_{xx3} + \sigma_{xy3}\delta\gamma_{xy3}\right) dV.
\end{aligned} \tag{17}$$

Substituting Eq. (1) in Eq. (17) one obtains:

$$\begin{aligned}
\delta T_i = & -\int_L \left\{ \delta u_i \left[\left(I_0^{(i)} + \frac{2I_1^{(i)}}{R_i} + \frac{I_2^{(i)}}{R_i^2} \right) \ddot{u}_i - \left(I_1^{(i)} + \frac{I_2^{(i)}}{R_i} \right) \ddot{\theta}_i \right] \right\} dx - \\
& -\int_L \left\{ \delta\theta_i \left[I_2^{(i)}\ddot{\theta}_i - \left(I_1^{(i)} + \frac{I_2^{(i)}}{R_i} \right) \ddot{u}_i \right] + \delta v \left(I_0^{(i)}\ddot{v} \right) \right\} dx \quad \forall i = 1,2,3,
\end{aligned} \tag{18}$$

$$\delta U_i = \int_L \left\{ \delta\varepsilon_{D1i} \left[J_0^{(i)}\varepsilon_{D1i} + J_1^{(i)}\varepsilon_{D2i} \right] + \delta\varepsilon_{D2i} \left[J_2^{(i)}\varepsilon_{D2i} + J_1^{(i)}\varepsilon_{D1i} \right] \right\} dx \quad \forall i = 1,2, \tag{19}$$

$$\delta U_3 = \int_L \left\{ \delta\varepsilon_{D13} \left(J_0^{(3)}\varepsilon_{D13} \right) + \delta\varepsilon_{D23} \left(J_2^{(3)}\varepsilon_{D23} \right) + \delta\varepsilon_{D33} \left(J_3^{(3)}\varepsilon_{D33} \right) \right\} dx. \tag{20}$$

It should be soundly noted that for the sake of algebraic simplicity Eq. (20) is obtained from δU_3 of Eq. (17) by assuming the core with elastic behavior (this implies a relaxation time with value zero). The purpose of this handing in the inner layer lies in the possibility to model also a sandwiched curved beam with elastic behavior as a limiting case of the present development. However, in order to complete the description of the viscoelastic behavior of the core, Eq. (20) will be reconsidered afterwards within the finite element context, taking into account the concepts of Section 2.4.

The coefficients of Eq. (18) and Eq. (19) are defined in the following form

$$\left\{ I_0^{(i)}, I_1^{(i)}, I_2^{(i)} \right\} = b \int_{l_{ai}}^{l_{bi}} \rho_i \left\{ 1, (y - y_i), (y - y_i)^2 \right\} dy \quad \forall i = 1,2,3, \tag{21}$$

$$\left\{ J_0^{(i)}, J_1^{(i)}, J_2^{(i)} \right\} = b \int_{l_{ai}}^{l_{bi}} E_i \left\{ 1, (y - y_i), (y - y_i)^2 \right\} dy \quad \forall i = 1,2. \tag{22}$$

The limits of these integrals, l_{ai} and l_{bi} can be easily deduced from Figure 2, the values of y_i, $i = 1,2,3$ as well; whereas b is the width of the beam, ρ_i is the mass density of each layer, E_i means the modulus of elasticity of each elastic layers. The coefficients $J_0^{(3)}$ and $J_2^{(3)}$ can be calculated appealing to Eq. (22) with the geometric and material properties corresponding to the core layer, whereas $J_3^{(3)}$ can be calculated as:

$$J_3^{(3)} = k_3 G_3 h_3 b \tag{23}$$

Note that Eq. (23) can be interpreted as the conventional shear rigidity of the Timoshenko beam, where G_3 and k_3 are the transverse modulus of elasticity and the shear coefficient, respectively.

4 FINITE ELEMENT FORMULATION

4.1 Basic formulation

Finite Element models can be constructed through discretization of the Hamilton principle given in Eq. (15). The finite element is formulated by discretizing the generalized displacements $\bar{u}$ and $\tilde{u}$ given in Eq. (4) and the bending displacement v in the following form:

$$\begin{aligned} \bar{u} &= \mathbf{N}_1 \mathbf{q}_e, \\ v &= \mathbf{N}_2 \mathbf{q}_e, \\ \tilde{u} &= \mathbf{N}_3 \mathbf{q}_e, \end{aligned} \tag{24}$$

where:

$$\begin{aligned} \mathbf{q}_e &= \left[\bar{u}_1, v_1, v_1', \tilde{u}_1, \bar{u}_2, v_2, v_2', \tilde{u}_2\right]^T, \\ \mathbf{N}_1 &= \left[F_1, 0, 0, 0, F_2, 0, 0, 0\right], \\ \mathbf{N}_2 &= \left[0, F_3, F_4, 0, 0, F_5, F_6, 0\right], \\ \mathbf{N}_3 &= \left[0, 0, 0, F_1, 0, 0, 0, F_2\right], \end{aligned} \tag{25}$$

and

$$\begin{aligned} F_1 = 1-\zeta, \qquad & F_2 = \zeta, \\ F_3 = 1-3\zeta^2+2\zeta^3, \qquad & F_4 = L_e\zeta(\zeta-1)^2, \\ F_5 = \zeta^2(3-2\zeta), \qquad & F_6 = L_e\zeta^2(\zeta-1), \\ \zeta = x/L_e. & \end{aligned} \tag{26}$$

L_e is the length of the element.

Thus, the finite element representation of displacements and rotations of the layers given in Eq. (5), can be written as:

$$\begin{aligned} u_1 = \mathbf{N}_{11}\mathbf{q}_e, \qquad & \theta_1 = \mathbf{N}_2'\mathbf{q}_e, \\ u_2 = \mathbf{N}_{21}\mathbf{q}_e, \qquad & \theta_2 = \mathbf{N}_2'\mathbf{q}_e, \\ u_3 = \mathbf{N}_{31}\mathbf{q}_e, \qquad & \theta_3 = \mathbf{N}_{32}\mathbf{q}_e, \\ v = \mathbf{N}_2\mathbf{q}_e, & \end{aligned} \tag{27}$$

where:

$$\begin{aligned} \mathbf{N}_{11} &= \left[F_1, 0, 0, F_1/2, F_2, 0, 0, F_2/2\right], \\ \mathbf{N}_{21} &= \left[F_1, 0, 0, -F_1/2, F_2, 0, 0, -F_2/2\right], \\ \mathbf{N}_{31} &= \left[\eta_a F_1, \eta_o F_3', \eta_o F_4', -\eta_b F_1, \eta_a F_2, \eta_o F_5', \eta_o F_6', -\eta_b F_2\right], \\ \mathbf{N}_{32} &= \left[\eta_d F_1, \eta_e F_3', \eta_e F_4', -\eta_c F_1, \eta_d F_2, \eta_e F_5', \eta_e F_6', -\eta_c F_2\right]. \end{aligned} \tag{28}$$

The membranal (ε_{D1i}, i=1,2,3), bending (ε_{D2i}, i=1,2) and shear (ε_{D33}) components of strain can be written in the following discretized form:

$$\begin{aligned} \varepsilon_{D11} = \mathbf{B}_{11}\mathbf{q}_e, \qquad & \epsilon_{D21} = \mathbf{B}_{21}\mathbf{q}_e, \\ \varepsilon_{D12} = \mathbf{B}_{12}\mathbf{q}_e, \qquad & \epsilon_{D22} = \mathbf{B}_{22}\mathbf{q}_e, \\ \varepsilon_{D13} = \mathbf{B}_{13}\mathbf{q}_e, \qquad & \epsilon_{D23} = \mathbf{B}_{23}\mathbf{q}_e, \\ \varepsilon_{D33} = \mathbf{B}_{33}\mathbf{q}_e, & \end{aligned} \tag{29}$$

where:

$$\begin{gathered}\mathbf{B}_{11}=\frac{\mathbf{N}_1'}{L_e}+\frac{\mathbf{N}_3'}{2L_e}+\frac{\mathbf{N}_2}{R_1},\quad \mathbf{B}_{12}=\frac{\mathbf{N}_1'}{L_e}-\frac{\mathbf{N}_3'}{2L_e}+\frac{\mathbf{N}_2}{R_2},\\ \mathbf{B}_{21}=-\frac{\mathbf{N}_2''}{L_e^2}+\left(\frac{\mathbf{N}_1'}{L_e}+\frac{\mathbf{N}_3'}{2L_e}\right)\frac{1}{R_1},\quad \mathbf{B}_{22}=-\frac{\mathbf{N}_2''}{L_e^2}+\left(\frac{\mathbf{N}_1'}{L_e}-\frac{\mathbf{N}_3'}{2L_e}\right)\frac{1}{R_2},\\ \mathbf{B}_{13}=\frac{\eta_a\mathbf{N}_1'}{L_e}-\frac{\eta_b\mathbf{N}_3'}{L_e}+\frac{\eta_o\mathbf{N}_2''}{L_e^2}+\frac{\mathbf{N}_2}{R_3},\\ \mathbf{B}_{23}=\frac{\eta_c\mathbf{N}_3'}{L_e}-\frac{\eta_k\mathbf{N}_1'}{L_e}+\frac{\eta_l\mathbf{N}_2''}{L_e^2},\quad \mathbf{B}_{33}=\eta_f\mathbf{N}_1-\eta_g\mathbf{N}_3+\frac{\eta_h\mathbf{N}_2'}{L_e}.\end{gathered}\tag{30}$$

In Eq. (28) and Eq. (30) the following definitions have been introduced:

$$\begin{gathered}\eta_a=1-\frac{h_1}{4R_1}+\frac{h_2}{4R_2},\quad \eta_b=\frac{h_1}{8R_1}+\frac{h_2}{8R_2},\quad \eta_c=\frac{\eta_a}{h_3},\quad \eta_d=\frac{4\eta_b}{h_3}+\frac{1}{R_3},\\ \eta_e=-\frac{\bar{h}}{h_3}+\frac{\tilde{h}}{4R_3},\quad \eta_f=-\eta_d,\quad \eta_g=\eta_c,\quad \eta_k=\frac{\eta_b}{h_3},\\ \eta_h=1+\frac{\bar{h}}{h_3}-\frac{\tilde{h}}{R_3},\quad \eta_l=\frac{\bar{h}}{h_3},\quad \eta_o=\frac{\tilde{h}}{4}.\end{gathered}\tag{31}$$

Now substituting Eq. (27) in Eq. (18) one obtains the variation of the kinetic energy of the finite element:

$$\delta T=-\delta\mathbf{q}_e^T\mathbf{M}_e\ddot{\mathbf{q}}_e\tag{32}$$

where $\mathbf{M}_e$ is the elementary mass matrix given by:

$$\mathbf{M}_e=\mathbf{M}_{e1}+\mathbf{M}_{e2}+\mathbf{M}_{e3}\tag{33}$$

in which $\mathbf{M}_{e1}$, $\mathbf{M}_{e2}$ and $\mathbf{M}_{e3}$ are the mass contributions of the three layers which can be written in the following form:

$$\begin{gathered}\mathbf{M}_{e1}=\int_0^1\left[I_x^{(1)}\mathbf{N}_{11}^T\mathbf{N}_{11}+I_0^{(1)}\mathbf{N}_2^T\mathbf{N}_2-\frac{I_{xr}^{(1)}}{L_e}\left(\mathbf{N}_{11}^T\mathbf{N}_2'+\mathbf{N}_2'^T\mathbf{N}_{11}\right)+\frac{I_2^{(1)}}{L_e^2}\mathbf{N}_2'^T\mathbf{N}_2'\right]L_e d\zeta,\\ \mathbf{M}_{e2}=\int_0^1\left[I_x^{(2)}\mathbf{N}_{21}^T\mathbf{N}_{21}+I_0^{(2)}\mathbf{N}_2^T\mathbf{N}_2-\frac{I_{xr}^{(2)}}{L_e}\left(\mathbf{N}_{21}^T\mathbf{N}_2'+\mathbf{N}_2'^T\mathbf{N}_{21}\right)+\frac{I_2^{(2)}}{L_e^2}\mathbf{N}_2'^T\mathbf{N}_2'\right]L_e d\zeta,\\ \mathbf{M}_{e3}=\int_0^1\left[I_x^{(3)}\mathbf{N}_{31}^T\mathbf{N}_{31}+I_0^{(3)}\mathbf{N}_2^T\mathbf{N}_2+I_2^{(3)}\mathbf{N}_{32}^T\mathbf{N}_{32}\right]L_e d\zeta,\end{gathered}\tag{34}$$

where in order to contract notation $I_x^{(i)}$ and $I_{xr}^{(2)}$ are defined as follows:

$$\begin{aligned}I_x^{(i)}&=I_0^{(i)}+\frac{2I_1^{(i)}}{R_i}+\frac{I_2^{(i)}}{R_i^2}\Bigg)\quad\forall i=1,2,3,\\ I_{xr}^{(i)}&=I_1^{(i)}+\frac{I_2^{(i)}}{R_i}\Bigg)\quad\forall i=1,2.\end{aligned}\tag{35}$$

The elementary stiffness matrix can be obtained substituting Eq. (27) and Eq. (29) into Eq. (19). It should be remembered that Eq. (20) was obtained under the assumption of elastic core. Then, the variation of the internal energy of the finite element is:

$$\delta U_e = \delta \mathbf{q}_e^T \mathbf{K}_e \mathbf{q}_e \tag{36}$$

Thus, the elementary stiffness matrix $\mathbf{K}_e$, in the limiting case of the inner layer behaving elastically, can be written as:

$$\mathbf{K}_e = \mathbf{K}_{e1} + \mathbf{K}_{e2} + \mathbf{K}_{e3} \tag{37}$$

where:

$$\begin{aligned}
\mathbf{K}_{e1} &= \int_0^1 \left[J_0^{(1)} \mathbf{B}_{11}^T \mathbf{B}_{11} + J_1^{(1)} \left(\mathbf{B}_{11}^T \mathbf{B}_{21} + \mathbf{B}_{21}^T \mathbf{B}_{11} \right) + J_2^{(1)} \mathbf{B}_{21}^T \mathbf{B}_{21} \right] L_e d\zeta, \\
\mathbf{K}_{e2} &= \int_0^1 \left[J_0^{(2)} \mathbf{B}_{12}^T \mathbf{B}_{12} + J_1^{(2)} \left(\mathbf{B}_{12}^T \mathbf{B}_{22} + \mathbf{B}_{22}^T \mathbf{B}_{12} \right) + J_2^{(2)} \mathbf{B}_{22}^T \mathbf{B}_{22} \right] L_e d\zeta, \\
\mathbf{K}_{e3} &= \int_0^1 \left[J_0^{(3)} \mathbf{B}_{13}^T \mathbf{B}_{13} + J_2^{(3)} \mathbf{B}_{23}^T \mathbf{B}_{23} + J_3^{(3)} \mathbf{B}_{33}^T \mathbf{B}_{33} \right] L_e d\zeta.
\end{aligned} \tag{38}$$

However, as the core is viscoelastic, the σ_{x3} and σ_{xy3} of Eq. (17) are no longer time independent, consequently the stiffness matrix component $\mathbf{K}_{e3}$ (that was derived in this section assuming the core with elastic behavior) has to be reformulated in view of the concepts introduced in Section 2.4.

Finally the virtual work of the external forces of the finite element is given by:

$$\delta W_e = \delta \mathbf{q}_e^T \mathbf{F}_e \tag{39}$$

4.2 Finite element description of the viscoelastic core

The operator of the fractional derivative defined in Eq. (13) can be approximated by several procedures, for example the Grünwald approximation (see: Grünwald (1867)). There is also a numerical method based on the Gear scheme for the approximation of fractional derivatives in the context of finite differences methods, as one can see in the work of Galucio et al. (2006). The Grünwald procedure is adopted here since, being valid for all values of α, it is easy to implement in a finite elements procedure. Thus, the finite difference approximation of the Grünwald definition is given by:

$$\frac{d^\alpha f(t)}{dt^\alpha} \approx \left(\Delta t \right)^{-\alpha} \sum_{j=0}^{N_t} A_{j+1} \, f\left(t - j\Delta t \right) \tag{40}$$

where Δt is the time step increment of the numerical scheme. The upper limit of the sum N_t is strictly lower than N, and A_{j+1} represents the Grünwald coefficients given either in terms of the gamma function or by the recurrence formulae, that is:

$$A_{j+1} = \frac{\Gamma(j-\alpha)}{\Gamma(-\alpha)\Gamma(j+1)} \qquad \text{or} \qquad A_{j+1} = \frac{j-\alpha-1}{j} A_j \tag{41}$$

Now the following strain function as internal variable is introduced:

$$\bar{\varepsilon} = \varepsilon - \frac{\sigma}{E_\infty} \tag{42}$$

such that the constitutive model described in Eq. (12) can be rewritten as:

$$\bar{\varepsilon} + \tau^\alpha \frac{d^\alpha \bar{\varepsilon}}{dt^\alpha} = \frac{E_\infty - E_o}{E_\infty}\varepsilon \tag{43}$$

This change of the strain variable leads to the presence of only one fractional derivative operator in the constitutive expression of Eq. (43) instead of the two fractionary operators in Eq. (12). Using the Grünwald approximations, i.e., substituting Eq. (40) in Eq. (43), and taking into account that $A_1 = 1$, it is possible to arrive to the following discretized form of the constitutive relation:

$$\bar{\varepsilon}^{(n+1)} = (1-c)\frac{E_\infty - E_o}{E_\infty}\varepsilon^{(n+1)} - c\sum_{j=1}^{N_t} A_{j+1}\bar{\varepsilon}^{(n+1-j)} \tag{44}$$

where c is a dimensionless constant given by

$$c = \frac{\tau^\alpha}{\tau^\alpha + \Delta t^\alpha} \tag{45}$$

It should be mentioned that the Grünwald coefficients in Eq. (44), which are strictly decreasing when j increases, describe the fading memory phenomena. In other words, the behavior of the viscoelastic material at a given time step depends more strongly on the recent time history than on the distant one (see Galucio et al. (2004)).

Now the variation of the axial and shear stress of the core can be defined from the definition anelastic strain in Eq. (42) and considering its discretized form in Eq. (42). Thus, remembering assumption (4) one obtains for the viscoelastic core:

$$\sigma_{i3}^{(n+1)} = E_\infty\left(\varepsilon_{i3}^{(n+1)} - \bar{\varepsilon}_{i3}^{(n+1)}\right) \tag{46}$$

or in extended form:

$$\begin{aligned}
\sigma_{x3}^{(n+1)} &= E_3\left[\left(1 + c\frac{E_\infty - E_o}{E_\infty}\right)\varepsilon_{x3}^{(n+1)} + c\frac{E_\infty}{E_o}\sum_{j=1}^{N_t} A_{j+1}\bar{\varepsilon}_{x3}^{(n+1-j)}\right] \\
\sigma_{xy3}^{(n+1)} &= G_3\left[\left(1 + c\frac{E_\infty - E_o}{E_\infty}\right)\gamma_{xy3}^{(n+1)} + c\frac{E_\infty}{E_o}\sum_{j=1}^{N_t} A_{j+1}\bar{\gamma}_{xy3}^{(n+1-j)}\right]
\end{aligned} \tag{47}$$

where E_3 and G_3 are the longitudinal and shear elastic moduli of the viscoelastic core that can be written in terms of the relaxed modulus E_o as follows:

$$E_3 = E_o, \qquad G_3 = G_o = \frac{E_o}{2\,(1+\nu)} \tag{48}$$

In order to derive the expression of the stiffness matrix of the core layer accounting for the viscoelastic behavior, one should recall the definitions of the axial and shear strains of the

core given in Eq. (8) and Eq. (11). Then taking into account Eq. (33) the finite element representation of the viscoelastic strain components can be written in following form:

$$\begin{aligned} \varepsilon_{x3}^{(n+1)} &= \left(\mathbf{B}_{13} - y\mathbf{B}_{23}\right)\mathbf{q}_e^{(n+1)} \\ \gamma_{xy3}^{(n+1)} &= \mathbf{B}_{33}\mathbf{q}_e^{(n+1)} \end{aligned} \tag{49}$$

The anelastic strains $\bar{\varepsilon}_{x3}^{(n+1)}$ and $\bar{\gamma}_{xy3}^{(n+1)}$ can be obtained with the same form given in Eq. (49) but in terms of the discretized anelastic unknowns $\bar{\mathbf{q}}_e^{(n+1)}$. These unknowns depend on the displacement history and are updated using the following expression:

$$\bar{\mathbf{q}}_e^{(n+1)} = (1-c)\,\frac{E_\infty - E_o}{E_\infty}\mathbf{q}_e^{(n+1)} - c\sum_{j=1}^{N_t} A_{j+1}\bar{\mathbf{q}}_e^{(n+1-j)} \tag{50}$$

Thus, taking into account Eq. (49) and Eq. (50) the stresses of the Eq. (47) can be written as:

$$\begin{aligned} \sigma_{x3}^{(n+1)} &= E_3\left(\mathbf{B}_{13} - y\mathbf{B}_{23}\right)\left[\left(1 + c\frac{E_\infty - E_o}{E_\infty}\right)\mathbf{q}_e^{(n+1)} + c\frac{E_\infty}{E_o}\sum_{j=1}^{N_t} A_{j+1}\bar{\mathbf{q}}_e^{(n+1-j)}\right] \\ \sigma_{xy3}^{(n+1)} &= G_3\mathbf{B}_{33}\left[\left(1 + c\frac{E_\infty - E_o}{E_\infty}\right)\mathbf{q}_e^{(n+1)} + c\frac{E_\infty}{E_o}\sum_{j=1}^{N_t} A_{j+1}\bar{\mathbf{q}}_e^{(n+1-j)}\right] \end{aligned} \tag{51}$$

Now concerning the internal energy (see Eq. (17)) of the viscoelastic core and employing Eq. (51) one has in the domain of the finite element the following expression:

$$\begin{aligned} \int_{V_e}\left[\left(\mathbf{B}_{13}^T - y\mathbf{B}_{23}^T\right)\sigma_{x3}^{(n+1)} + \mathbf{B}_{33}^T\sigma_{xy3}^{(n+1)}\right]dV = \left(1 + c\frac{E_\infty - E_o}{E_\infty}\right)\mathbf{K}_{e3}\mathbf{q}_e^{(n+1)} + \\ c\frac{E_\infty}{E_o}\mathbf{K}_{e3}\sum_{j=1}^{N_t} A_{j+1}\bar{\mathbf{q}}_e^{(n+1-j)} \end{aligned} \tag{52}$$

From Eq. (52) one can obtain the stiffness matrix component of the curved finite element with the viscoelastic core. Notice that $\mathbf{K}_{e3}$ is the stiffness matrix component of the core defined in Eq. (38).

4.3 Discretized equations of motion and algorithm implementation

Once the elementary mass and stiffness matrices are completely formulated, after putting together Eq. (32), Eq. (36), Eq. (39), Eq. (52) and performing some algebraic handling one obtains the elementary equation of motion as:

$$\mathbf{M}_e\ddot{\mathbf{q}}_e^{(n+1)} + \left(\mathbf{K}_e + \bar{\mathbf{K}}_{e3}\right)\mathbf{q}_e^{(n+1)} = \mathbf{F}_e^{(n+1)} + \bar{\mathbf{F}}_e^{(n+1)} \tag{53}$$

where $\mathbf{M}_e$ and $\mathbf{K}_e$ are the mass matrix and the stiffness matrix of the element as defined in Eq. (39) and Eq. (52). The modified stiffness matrix $\bar{\mathbf{K}}_{e3}$ and loading vector $\bar{\mathbf{F}}_e^{(n+1)}$ that appear

from the viscoelastic behavior of the inner layer, are given by:

$$\begin{aligned} \bar{\mathbf{K}}_{e3} &= c\frac{E_\infty - E_o}{E_\infty}\mathbf{K}_{e3} \\ \bar{\mathbf{F}}_e^{(n+1)} &= -c\frac{E_\infty}{E_o}\mathbf{K}_{e3}\sum_{j=1}^{N_t} A_{j+1}\bar{\mathbf{q}}_e^{(n+1-j)} \end{aligned} \tag{54}$$

It is interesting to note that Eq. (53) contains in a unified fashion the cases of sandwich beams with viscoelastic core or elastic core. For the case of elastic core $\bar{\mathbf{K}}_{e3}$ and $\bar{\mathbf{F}}_e^{(n+1)}$ vanish since the dimensionless constant $c = 0$, consequently Eq. (53) is reduced to a classical equation of motion.

Appealing to the common assembly procedure Eq. (53) becomes in:

$$\mathbf{M}\ddot{\mathbf{Q}}^{(n+1)} + \left(\mathbf{K} + \bar{\mathbf{K}}_3\right)\mathbf{Q}^{(n+1)} = \mathbf{F}^{(n+1)} + \bar{\mathbf{F}}^{(n+1)} \tag{55}$$

where $\mathbf{M}$ and $\mathbf{K}$ are the global mass and stiffness matrices, respectively. $\bar{\mathbf{K}}_3$ is the global stiffness matrix of the viscoelastic core, $\mathbf{Q}$ is the global vector of degrees of freedom, and $\mathbf{F}$ is the global loading vector and $\bar{\mathbf{F}}$ is the global modified loading vector. Super-indexes in the previous equations intend for the n^{th} calculation step.

In order to implement the algorithm for calculation of transient dynamics, the Newmark method is employed. However some changes in the classical Newmark scheme should be carried out in order to tackle the problem of the viscoelastic core modeled with fractional calculus (Deü et al., 2003; Galucio et al., 2004). For detailed descriptions the reader should see the work of Deü et al. (2003). Thus, in Figure 4 one can see a flux diagram of the resolution algorithm.

5 NUMERICAL ANALYSIS AND PARAMETRIC STUDIES

5.1 Validation and comparison of the present model

In this section numerical computations are performed in order to validate and compare the model with other studies of the international literature.

The first example corresponds to a simply supported straight viscoelastic Timoshenko beam (Chen, 1995; Galucio et al., 2004). This implies to set, in the present model, $R \to \infty$ and to eliminate the influence of the external layers (or simply set $h_1 = h_2 = 0$). The length, width and height of the beam are $L = 10\ m$, $b = 2\ m$ and $h_3 = 50\ cm$. The shear coefficient of the beam is defined by $k_3 = 10(1+\nu)/(12+11\nu)$. The beam is modeled with 50 finite elements with an external uniform step loading of $F_E = 10\ \mathcal{H}(t)\ N/m$ on its top side. $\mathcal{H}(t)$ is the Heaviside step function. The viscoelastic material is characterized by means of the following properties: $E_o = 19.6\ MPa$, $E_\infty = 98\ MPa$, $\rho = 500\ kg/m^3$, $\nu = 0.3$ and $\tau = 2.24\ s$.

In Figure 5 the time-dependent displacements at the center of the beam for a standard solid model ($\alpha = 1.00$) and for a fractional derivative one ($\alpha = 0.75$ and $\alpha = 0.50$) are shown. In this Figure the responses obtained with the present approach and with the approach of Galucio et al. (2004) are compared. As one can see both responses are in well agreement.

The second example corresponds to a sandwich shallow arc. The arc is composed by a viscoelastic core (specimen of 3M$^{(TM)}$ number ISD112 at 27°) with a thickness of $5\ mm$ bounded by metallic (aluminium) layers with thickness of $2.5\ mm$. The width of the arc is $b = 20\ mm$ the curvature radius and the subtended arc are $R = 2.525\ m$ and $\Phi = 0.4\ rad$. The mechanical characteristics for the elastic faces are $\rho = 2690\ kg/m^3$, $\nu = 0.345$ and $E = 70.3 \times 10^3 MPa$. The mass density and Poisson coefficient of the viscoelastic material are $\rho = 1600 kg/m^3$ and

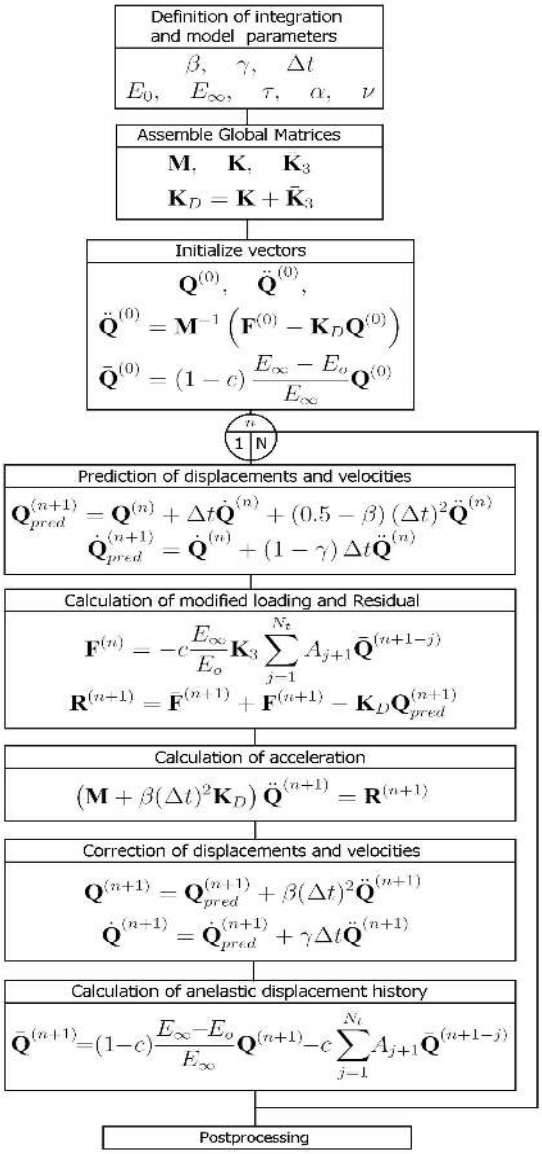

Figure 4: Flow-chart of the modified Newmark method.

$\nu = 0.5$, whereas the material parameters for the fractional derivative viscoelastic model are identified (Galucio et al., 2004) as $E_o = 1.5\ MPa$, $E_\infty = 69.9495\ MPa$, $\alpha = 0.7915$ and $\tau = 1.4052 \times 10^{-2}\ ms$. The arc modeled with fifty finite elements is subjected to a unitary Heaviside step flexural point load located at the center of the arc and directed towards the center of curvature.

In Figure 6 one can see the radial displacement of the node where the load is placed. The response obtained with curved elements is tested with a frame model of straight sandwich beam elements (Deü et al., 2003; Galucio et al., 2004) programmed ad-hoc. It is possible to note the agreement between both approaches. It should be mentioned that both approaches converge monotonically to the same values as the number of elements in the models are increased. Although the frame approach proved to be faster than the arc approach, this aspect may be associated with the shape functions employed here for the arc. These shape functions can be replaced in the arc element in order to improve approximations and accelerate the convergence.

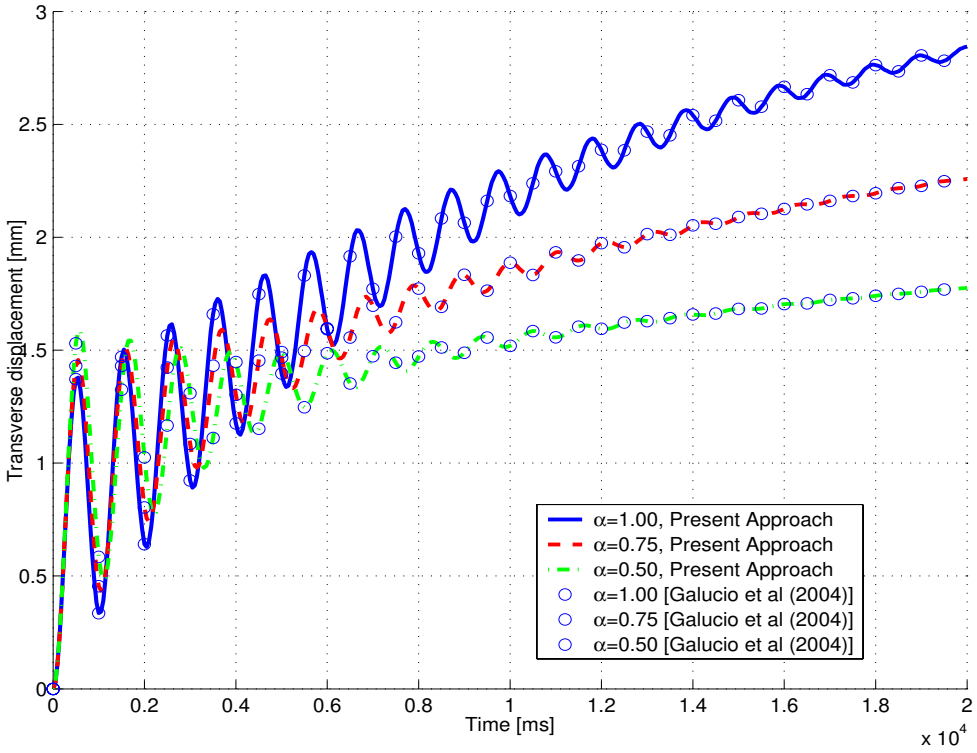

Figure 5: Comparison of displacements at the center of the beam.

However this is matter of future extensions.

5.2 Parametric studies on the dynamics of sandwich curved beams

In this section some parametric studies are carried out in order to characterize the dynamics of curved viscoelastic sandwich beams. In Figure 7 one can see a sketch of a shallow curved beam with clamped ends. The horizontal distance L_h between the geometric centers of the clamped ends is a constant while the shallowness parameter Δ_R can vary form zero (i.e. a straight beam) to a certain value in terms of a percentage of L_R, normally no longer than 20%.

The first example of this section corresponds to a fully viscoelastic arc. The width and height of the beam are $b = 2\ m$ and $h_3 = 50\ cm$. The horizontal distance is $L_h = 10\ m$. Since this example is suited only for viscoelastic arcs, the influence of elastic external layers is eliminated (i.e. $h_1 = h_2 = 0$). The properties of the viscoelastic material are: $E_o = 19.6\ MPa$, $E_\infty = 98\ MPa$, $\rho = 500\ kg/m^3$, $\nu = 0.3$ and $\tau = 2.24\ s$. The shear coefficient of the beam is defined by $k_3 = 10(1+\nu)/(12+11\nu)$. The beam is subjected to an outward radial and uniform step-load of $F_E = 1000\mathcal{H}(t)\ N/m$. The curved arc is modeled with 100 finite elements, in order to have quite precise results.

In Figure 8 one can see the history of the radial displacement in the middle of the arc for the case where $\alpha = 0.5$ and for four different shallowness ratios. As one can see the transient oscillation period can be substantially diminished for the curved cases. In this last figure, an interesting aspect related to the relationship between the stationary response and arc dimensions can be also regarded. Note that as $\Delta_R/L_h \to 0$ (or $R \to \infty$) the length L of the curved beam (i.e. $L = R_3\Phi$, where Φ is the subtended angle) is such that $L \to L_h$. Thus with a small change in the length L with respect to the straight beam case ($L = L_h$) one gets an important reduction in the displacement response. For example, notice that for the case $\Delta_R/L_h = 0.05$

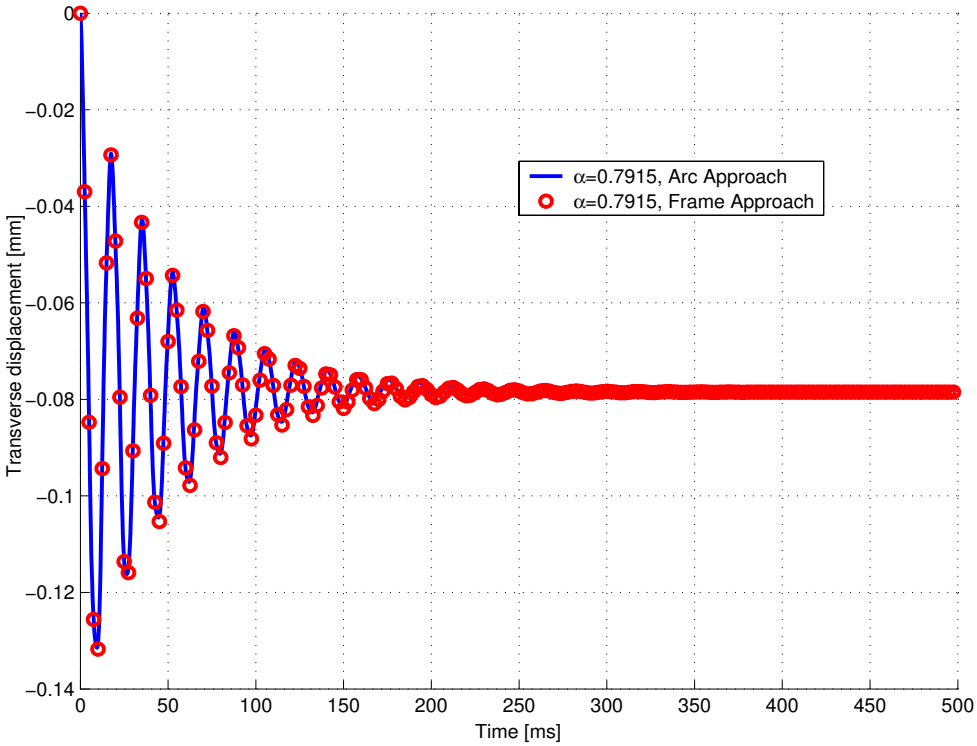

Figure 6: Comparison of displacements at the center of the shallow arc.

one can calculate the ratio arc length to L_h, that is $L/L_h = 1.0066$; in other words this means that with a slightly curved beam with an arc length less than 1% larger than the length of the straight beam one gets displacements that can be less than 50% of the corresponding values of the straight beam case (compare responses of $\Delta_R/L_h = 0$ and $\Delta_R/L_h = 0.05$ in Figure 8)

The second example of the transient behavior of sandwich curved beams corresponds to a shallow arc with a viscoelastic core (specimen of 3M$^{(TM)}$ number ISD112 at $27°$) bounded by aluminum layers. The material data for this calculation can be taken from the second example in the previous subsection. The fractional derivative order for the viscoelastic material is $\alpha = 0.79$. Considering once again Figure 7, the geometry of the structure is such that $L_h = 1\ m$ and $\Delta_R/L_h = 0.10$, the width is $b = 40\ mm$ and the height is $h = 20\ mm$ (i.e. $h = h_1 + h_2 + h_3$). The elastic external layers are such that $h_1 = h_2$. The structure is subjected to a radial step load

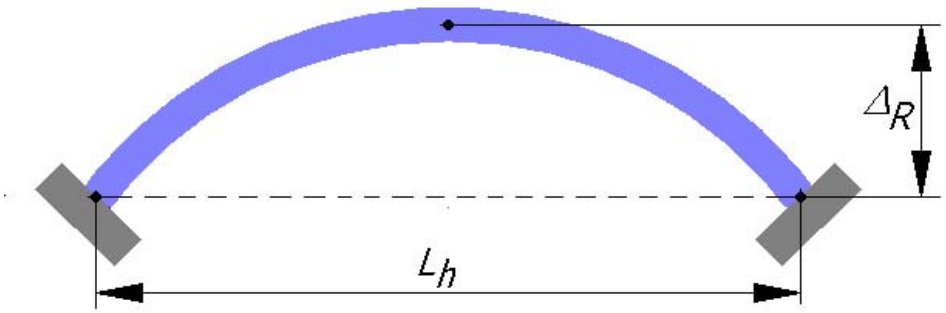

Figure 7: Geometric characterization of shallow circular arc.

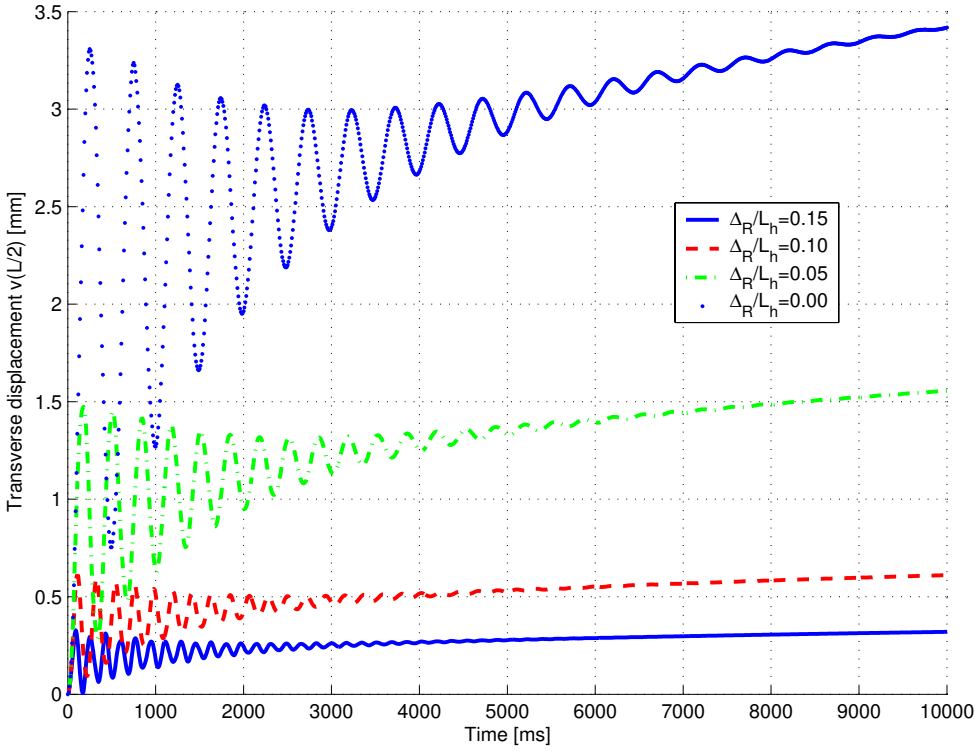

Figure 8: History of displacements at the center of the beam, for $\alpha = 0.5$ and different shallowness ratios Δ_R/L_h.

of value $F_E = 10\mathcal{H}(t)\ N$ located at center of the beam and directed outwards. The calculation is carried out over a period $T = 500\ ms$ which proved to be enough to reach a stationary constant response for all the analyzed cases. In this study the influence of the thickness of the viscoelastic core is analyzed.

In Figure 9 the time history of radial displacements at the loading point is depicted. The radial displacements of this figure are re-scaled by normalizing them with respect to the corresponding stationary radial displacement (i.e. $v(L/2,t)/v(L/2,t_{500})$), in order to have the same screen in all the cases, for comparative purposes. Thus, for a very thin ($h_3/h = 0.01$) viscoelastic layer it is possible to see a very short transient that ends after $40\ ms$, whereas for the other cases the transient periods are larger with a high oscillatory behavior.

6 CONCLUSIONS

In the present paper a model of sandwich curved beams with viscoelastic layer for transient dynamic analysis has been proposed. The structural model consist of three layers, where a viscoelastic core is bounded by two elastic layers. The behavior of the core has been described employing a four-parameters viscoelastic constitutive model defined in terms of fractional derivative operators of strains and stresses. The curved beam model has been numerically implemented in the context of the finite element method. Thereafter the constitutive model has been rearranged in order to be represented only in terms displacements. Thus only anelastic displacements had to be kept to represent the dynamics of the viscoelastic sandwich curved beam. The present model contains the straight beam and bar models as particular cases when the curvature radius is set to infinity (in practice to a large value). Numerical computations have been carried out to show the usefulness of the present approach as well as the transient behavior of the curved viscoelastic sandwich beams.

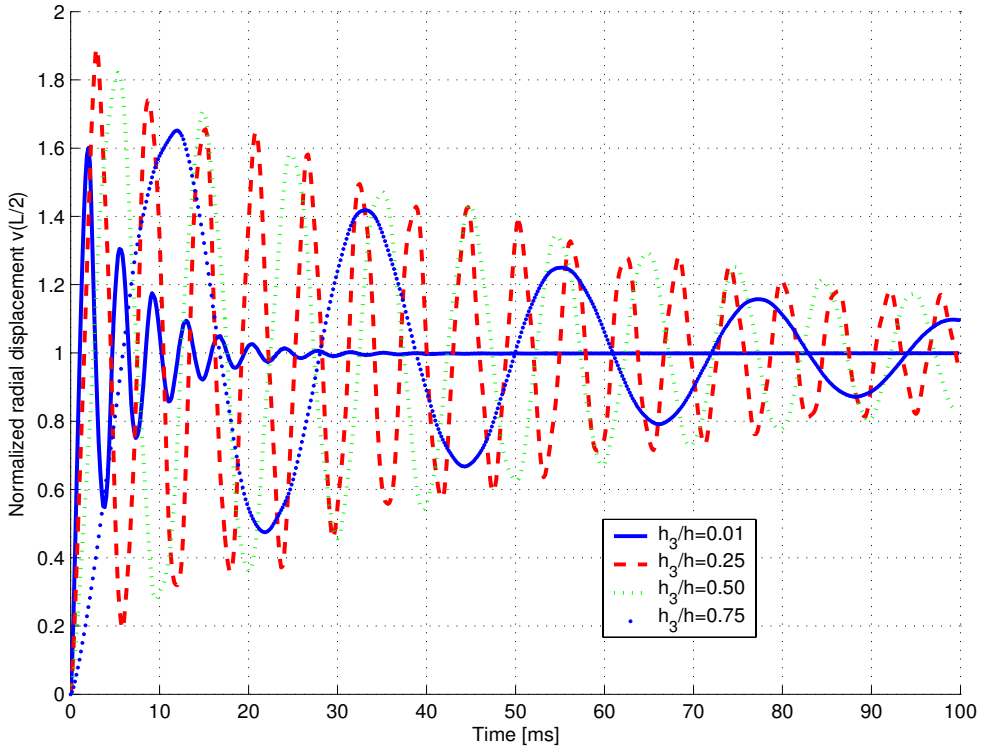

Figure 9: History of normalized displacements at the center of the beam, for $\alpha = 0.79$ and different ratios h_3/h.

REFERENCES

Baba B. and Thoppul S. Experimental evaluation of the vibration behavior of flat and curved sandwich composite beams with face/core debond. *Composite Structures*, 91:110–119, 2009.

Bagley R. and Torvik P. Fractional calculus - a different approach to the analysis of viscoelastically damped structures. *American Institute of Aircraft and Aeronautics*, 21:741–748, 1983.

Baz A. Boundary control of beams using active constrained layer damping. *Journal of Vibration and Acoustics*, 119:166–172, 1997.

Chen T.M. The hibrid laplace transform/finite element method applied to quasi-static and dynamic analysis of timoshenko beams. *International Journal for Numerical Methods in Engineering*, 38, 1995.

Coronado A., Trindade M., and Sampaio R. Frequency dependent viscoelastic models for passive viration isolation systems. *Shock and Vibration*, 9:253–264, 2002.

Deü J.F., Galucio A., and Ohayon R. *Finite element formulation for a transient dynamic analysis of viscoelastic beams using fractional derivative constitutive equations*. Oñate, E., Owen, D.R.J. Eds, Proceedings of VII International Conference on computational plasticity (CD-ROM), Barcelona, Spain, 2003.

Enelund M. and Jossefson A. Time-domain finite element analysis of viscoelastic structures with fractional derivatives constitutive relations. *American Institute of Aircraft and Aeronautics*, 35:1630–1637, 1997.

Galucio A., Deü J.F., Mengué S., and Dubois F. An adaptation of the gear scheme for fractional derivatives. *Computer Methods in applied Mechanics and Engineering*, 195:6073–6085, 2006.

Galucio A., Deü J.F., and Ohayon R. Finite element formulation of viscoelastic sandwich beams using fractional derivative operators. *Computational Mechanics*, 33:282–291, 2004.

Grünwald A. Über "begrenzte" derivationen and deren anwendung. *Zeitschrift für Mathematik und Physik*, 12:441–480, 1867.

Padovan J. Computational algorithms for fe formulations involving fractional operators. *Computational Mechanics*, 2:271–287, 1987.

Piovan M. and Cortínez V. Mechanics of thin-walled curved beams made of composite materials, allowing for shear deformability. *Thin Walled Structures*, 45, 2007.

Pritz T. Analysis of four-parameter fractional derivative model of real solid materials. *Journal of Sound and Vibration*, 195:103–115, 1996.

Sunsanto K. Vibration analysis of piezoelectric laminated slightly curved beams using distributed transfer function method. *International Journal of Solids and Structures*, 46:1564–1573, 2009.

Trindade M., Benjeddou A., and Ohayon R. Finite element modelling of hybrid active-passive vibration damping of multilayer piezoelectric sandwich beams - part i: Formulation. *International Journal for Numerical Methods in Engineering*, 51:835–854, 2001.